

# Cerebral Vasomotion: A 0.1-Hz Oscillation in Reflected Light Imaging of Neural Activity

JOHN E. W. MAYHEW,<sup>1</sup> STEPHEN ASKEW, YING ZHENG, JOHN PORRILL, G. W. MAX WESTBY,  
PETER REDGRAVE, DAVID M. RECTOR,\* AND RONALD M. HARPER\*

Artificial Intelligence Vision Research Unit, University of Sheffield, Sheffield, S10 2TP United Kingdom; and \*Department of Neurobiology, UCLA School of Medicine, 10833 Le Conte Avenue, Los Angeles, California 90095-1763

Received March 4, 1996.

**Imaging of scattered and reflected light from the surface of neural structures can reveal the functional architecture within large populations of neurons. These techniques exploit, as one of the principal signal sources, reflectance changes produced by local variation in blood volume and oxygen saturation related to neural activity. We found that a major source of variability in the captured light signal is a pervasive low-frequency (0.1-Hz) oscillation which apparently results from regional cerebral blood flow. This signal is present in brain parenchyma as well as the microvasculature and exhibits many characteristics of the low-frequency “vasomotion” signals observed in peripheral microcirculation. Concurrent measurements in brain with a laser Doppler flow meter contained an almost identical low-frequency signal. The presence of the 0.1-Hz oscillation in the cerebral microcirculation could underlie a portion of the previously described characteristics reported in reflected-light imaging studies. The prevalence of the oscillatory phenomena in the brain raises substantial temporal sampling issues for optical imaging and for other visualization techniques which depend on changes in regional cerebral blood dynamics, such as functional magnetic resonance imaging.** © 1996 Academic Press, Inc.

## INTRODUCTION

Imaging of reflected, transmitted, or scattered light as a measure of neural activity has been used for many years (Hill and Keynes, 1949) and has become increasingly popular for investigating the functional architecture of cortex and for obtaining high spatial resolution maps of cortical activity (Frostig *et al.*, 1990; Grinvald

*et al.*, 1988; Grinvald *et al.*, 1991). Changes in reflected and scattered light during neural activity result from a complex interaction of several processes. Increased neural activity produces both increased local blood flow and volume, differences in oxygen consumption, and changes in optical transmission characteristics of neural tissue (Cohen, 1973; Frostig *et al.*, 1990; Grinvald *et al.*, 1988, 1991; Lipton, 1973; MacVicar and Hochman, 1991; Poe *et al.*, 1994; Rector *et al.*, 1993; Tasaki and Byrne, 1994). These effects interact in a complex manner to change absorption and reflectance properties of underlying brain tissue and hence alter the observed spatiotemporal changes in light intensity collected from the imaged tissue.

The contribution of vascular signals to image data introduces the potential for “vascular artifacts” in optical signal data from neurones. Several investigators have adopted procedures to minimize such influences. The control procedures include averaging very large numbers (often thousands) of images to increase the signal/noise ratio (Blasdel and Salama, 1986; Grinvald *et al.*, 1991), focusing below the plane of the microvasculature (Ratzlaff and Grinvald, 1991; Ts’o *et al.*, 1990), and using analytic techniques of subtracting data collected under orthogonal stimulus conditions (Blasdel and Salama, 1986; Grinvald *et al.*, 1991). An important development of these methods is the recent work of Carmona *et al.* (1995), who attempted to remove the major effects of vascular artifacts using wavelet analysis.

Although these different procedures may variously ameliorate the visible effects of vascular artifacts in intrinsic signal data, it seemed important to examine them in somewhat more detail and to begin to identify and to characterize their spatial and temporal structure. To this end the present study analyzed long continuous data sequences from three different species and different brain structures to describe vascular contributions to optical signals.

<sup>1</sup> To whom correspondence should be addressed at AIVRU, University of Sheffield, Sheffield, S10 2TP UK. E-mail: J.E.W.Mayhew@aivru.sheffield.ac.uk.

## MATERIALS AND METHODS

### *Optical Imaging*

The camera system is composed of a 1.6-mm-diameter fiber optic conduit mounted on a charge-coupled device (CCD) array. To obtain images, the other end of the conduit is placed directly on the surface of the brain; the conduit has a spatial resolution of approximately 10  $\mu\text{m}$ . Light-emitting diodes (LEDs) of different wavelengths (570 and 660 nm) provide target illumination via an annulus of fibers surrounding the main bundle. Backscattered and reflected light from the tissue return to the camera through the image conduit. Details of construction and operation of this probe are described in Rector and Harper (1991). Image sequences were captured at 25 Hz, and a region corresponding to the area under the probe (typically  $150 \times 150$  pixels) was transferred to disk (at a frame rate of 25 Hz). On-line analysis provided experimental control and feedback to the experimenters.

### *Subjects and Experimental Procedures*

Reflectance imaging was carried out with both acute and unanesthetized preparations. In most experiments, anesthetized (urethane 1.3 g/kg) male Sprague-Dawley rats (280–320 g) bred in the Sheffield laboratory were used ( $N = 12$ ). After anesthesia induction, the animals were placed in a standard stereotaxic head frame (Kopf Instruments) and the dorsal surface of the skull and the dura were removed to expose the brain. Access to deep structures was gained by aspirating overlying tissue. Comparisons were made between the captured optical signals and those obtained from a laser Doppler flow (LDF) meter placed side-by-side on the surface of the neocortex; simultaneous recording was not possible due to light scatter from the LDF probe. The time series for both optical and LDF records were smoothed, the means removed, and the signals were scaled approximately to the same amplitude to facilitate comparison. The qualitative effects of a range of sensory stimuli on the reflectance optical signals were also determined. Noxious stimulation (a 5-s mechanical pinch approximately 70 g/mm<sup>2</sup>) was applied unilaterally to one of the hind paws. Visual stimulation was presented in the form of a flashing green LED (1 s on, 1 s off) positioned approximately 15 cm from the eye, while auditory stimulation was provided by gently tapping the ear bars of the head frame.

Effects of directly stimulating tissue from which optical signals were being recorded were also determined. In these experiments, the cerebral cortex and hippocampus overlying the right superior colliculus were removed unilaterally by aspiration. Approaching at an acute angle from the contralateral side of the brain in the coronal plane, a monopolar stimulating

microelectrode was positioned parallel to the dorsal surface of the collicular superficial layers 0.2–0.5 mm below the surface. The optical probe was then placed so that the tip of the stimulating electrode was positioned approximately at the center of the image. Optical responses of the superficial layers of the superior colliculus to direct electrical stimulation (10-s trains of 0.2-ms square wave pulses; 100 Hz; range 50–400  $\mu\text{A}$ ) were recorded. Finally, we tested the effects of administering local anesthetic (0.37 M procaine) (Dean *et al.*, 1982) to the surface of the superior colliculus on optical responses induced by electrical stimulation. All aspects of these experiments were performed with Home Office (UK) approval under Section 5(4) of the Animals (Scientific Procedures) Act 1986.

A sequence of images was also obtained in the UCLA laboratory from an unanesthetized cat prepared with a chronic implant which contained both the camera and an associated fiber optic conduit, together with electroencephalographic (EEG) recording electrodes. The optical probe was positioned on the dorsal surface of the hippocampus. A detailed description of the surgical details and experimental procedures associated with the collection of data have been published elsewhere (Poe *et al.*, 1994; Rector and Harper, 1991; Rector *et al.*, 1993). Briefly, an extensive series (>1 h) of continuous image data was collected while the cat alternated between periods of normal sleep and waking. All procedures were performed in compliance with the *Guide for the Care and Use of Laboratory Animals* (NIH Publication No. 86-23) and in facilities accredited by the American Association for Accreditation of Laboratory Animal Care (AAALAC). All experimental protocols received prior approval of the Institutional Animal Care and Use Committee.

Last, to determine if the optical recording system could detect the classic vasomotion signal (Colantuoni *et al.*, 1994), recordings were taken from human finger-nail pulp of one experimenter (Y.Z.).

### *Image Analysis*

The image capture and signal processing utilized a dedicated SGI Onyx (4x R4400 200-MHz processor) machine. The image capture and data analyses differed from most protocols reported for optical imaging (Blaedel and Salama, 1986; Bonhoeffer and Grinvald, 1993), in that our data sequences comprised continuous image-data streams of substantial duration. Typically, we captured a minimum of >1024 frames (41 s) at 25 Hz, with stimulus presentation usually after frame 512; however, the sequence from cat hippocampus was 10,000 frames (67 min). At the start of each experiment, the intensity of the LED providing target illumination, the frame grabber gain, and the dark level were adjusted to provide a mean image gray level of about 128 centered in the middle of the range and a standard

deviation that spanned about a sixth of the range. Thus, a gray level corresponded to about 1% of the mean signal, and when calibrated against the video signal voltage, one gray level corresponded to approximately 1.5 mV. The time series for each pixel was smoothed to remove higher-frequency components using a running window with a 0.95 (20-frame) forgetting factor and was averaged over the image to produce a single time series. Typically, in cases where the effects of sensory or electrical stimulation on optical signals were to be determined, the first 100 frames of the sequence were used to determine a mean gray level for each pixel. This value was subsequently subtracted from the corresponding pixel values in successive images to provide a measure of gray level change. Finally, Fourier spectra of each pixel from blocks of 1024 successive images from rat brain were averaged to determine optical activity related to heartbeat (approximately 5 Hz) and respiration (approximately 2 Hz).

## RESULTS AND DISCUSSION

The availability of extensive streams of continuous data enabled detection of the presence of a relatively broad band low-frequency modulation characteristically peaking around 0.1 Hz or 6 cycles/min. The signal is often as much as 1–2% of the gray level image; hence, it was necessary to run only a simple temporal smoothing algorithm to detect it (see Materials and Methods above).

In the absence of any form of stimulation, the 0.1-Hz signal was observed by placing the tip of the optical probe on the surface of a range of neural structures in the anesthetized rat, including cerebral cortex, striatum, thalamus, superior colliculus, inferior colliculus, and cerebellum. This signal was present in all structures and in all subjects that we have investigated ( $N = 12$  rats in this study and a further 30 animals used subsequently); moreover, we observed no differences between the signal recorded from the dural surface and that from a closed thin skull preparation. Successive measurements taken from the optical probe and an LDF meter (Perimed 4001), placed on adjacent regions of rat cerebral cortex, were almost indistinguishable (Fig. 1a). This finding shows that the two techniques measure, if not the same, then highly correlated, aspects of microcirculation (Fig. 1a). The patterns of variability in the vasomotion signal measured by the LDF meter and the low-frequency component of the optical signal were very similar (Fig. 1a). A low-frequency modulation of approximately 0.1 Hz in the regional cerebral blood flow using LDF has been widely reported (Dirnagl *et al.*, 1989; Golanov *et al.*, 1994; Morita *et al.*, 1995). This gives us confidence that our optical system and LDF are monitoring the same variation in hematocrit density (Fagrell *et al.*, 1980).

The 0.1-Hz signal is not a peculiarity of species or anesthetic state, since the signals were obtained from both the anesthetized rat and the hippocampus of an unanesthetized cat (Fig. 1b). The link between optical signals and changes in microcirculation was extended by the successful use of the optical probe to measure the classical vasomotion signal from the human fingernail pulp (Fig. 1c) (Sundberg, 1984). The 0.1-Hz signal was associated with some aspect of microcirculation which can be readily distinguished from other components in the images related to the cardiac and respiratory cycles. The Fourier spectrum of every pixel in a block of 1024 images was computed independently and averaged to reveal separate peaks of activity associated with heartbeat (5 Hz), breathing (2 Hz), and the low-frequency signal (0.1 Hz) (Fig. 1d).

For convenience, the low-frequency component of the optical signal is termed a "0.1-Hz oscillation"; however, the vasomotion signal contains a range of frequencies in the range 1–6 cycles/min (Sundberg, 1984). We also found the low-frequency modulation of the intrinsic optical signal to be a relatively broad band centered on 0.1 Hz. It appears reasonable, therefore, to conclude that a principal component of the intrinsic optical signal corresponds to an aspect of cerebral microcirculation which is commonly referred to as "vasomotion."

The current optical measurement of cerebral microcirculation provided an indication of both the temporal and spatial structure of dynamic changes. We emphasize that the 0.1-Hz signal was present in not only the arterial and venous systems, but also in the capillary beds of intervening regions of brain parenchyma (Fig. 2). The top left image in Fig. 2a shows the region ( $1.5 \times 1.5$  mm) from which optical measurements were taken; it contained branching arterioles (entering from top left), two principal venules (exiting bottom right), and intervening brain parenchyma. The remaining images in (a) represent a peristimulus montage of processed images (left to right, top to bottom sampled at 2-s intervals). The noxious pinch was applied at the beginning of the second row and was released between the second and third images (grayed background). Regional changes emerged in association with different elements in the image. We also found evidence of localized foci of 0.1-Hz activity about 100–200  $\mu\text{m}$  in diameter which showed interesting dynamics (Figs. 2a and 3c). These foci appeared as regions of larger-than-usual power in the low-frequency (temporal) spectrum. The phase differences in regional activation showed as apparent movement when the processed image sequence was animated. These phase relationships between pixels of different regions (see Fig. 2a) preclude simple explanations, such as general systemic or motion artifacts.

A further example of the spatial and temporal structure within the images was found in the time series

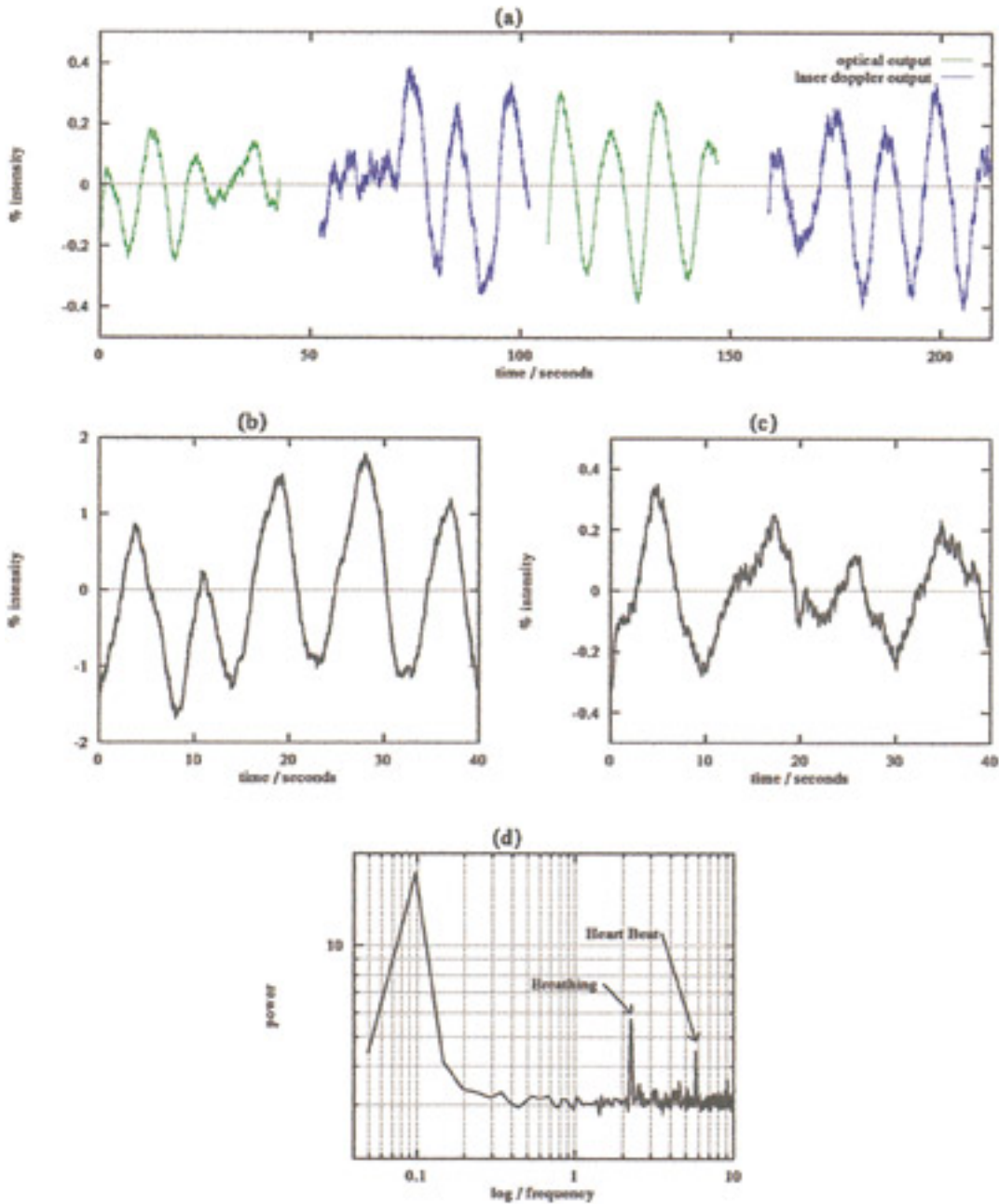
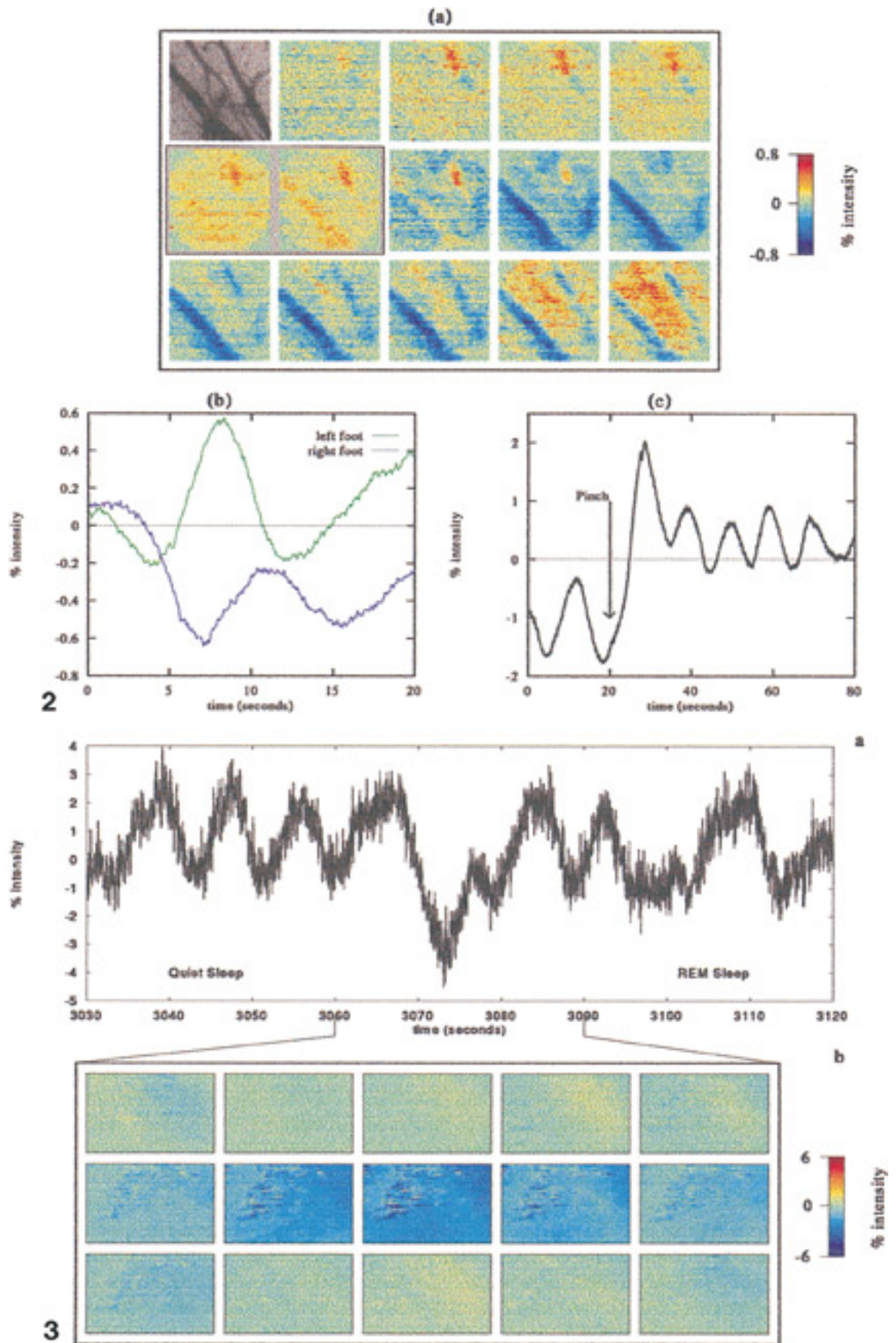


**FIG. 1.** Records from both optical probe and laser Doppler flow meter contained a low-frequency (0.1-Hz) oscillation. The 0.1-Hz signal can be distinguished from higher-frequency components attributable to cardiac and respiratory cycles. (a) Similar signals were present in alternating records from the optical probe and a laser Doppler flow meter. (b) Optical records from the hippocampus of an unanesthetized cat (Rector *et al.*, 1993) also contained the 0.1-Hz signal. The mean time series is plotted as a percentage of the mean gray level. (c) The classic 0.1-Hz vasomotion signal (Colantuoni *et al.*, 1994) was present in optical signals recorded from the back of the human fingernail (image processing described for (a) was applied). (d) Separate peaks of activity associated with heart beat (5 Hz), respiration (2 Hz), and the low-frequency signal (0.1 Hz) in averaged Fourier spectra of each pixel from a block of 1024 successive images from rat motor cortex.

recorded from an unanesthetized cat making transitions between different phases of sleep. The graph in Fig. 3 shows an example of the mean gray level changes in the optical record occurring during a transition between quiet sleep and rapid eye movement (REM) sleep. The montage represents individual frames cap-

tured every 2 s from the central 30 s of the record. Note first an area in the upper-right quadrant of the image which shows greater amplitude low-frequency oscillation than elsewhere and second a detailed spatial structure in the image during the transition. The source of these intriguing local variations is unknown.



We found that the low-frequency (0.1-Hz) oscillatory component of the optical signal was confounded with the effects of a range of variables acting on regional blood flow, including physiological state changes (Fig. 3), sensory stimulation (Figs. 2, 4a, and 4b), and direct electrical stimulation of the imaged tissue (Fig. 5). Effects on the signal can take the form of a change in amplitude of the 0.1-Hz oscillation (Figs. 2b and 2c), frequency (Fig. 2c), or an interruption of the 0.1-Hz cycle. Such changes are sometimes prolonged and can be accompanied by changes in the overall level of the signal (DC changes) which last several cycles of the 0.1-Hz oscillation (Fig. 2c).

The following results argue that the poststimulus increase in intensity of the signal arises, at least in part, from local changes in neural activity. These responses are superimposed on the background 0.1-Hz modulation, which appears to be omnipresent.

(i) The optical responses recorded from the left hindlimb motor area of rat cortex (Zilles and Wree, 1985; Neafsey *et al.*, 1986) differed reliably when a noxious pinch was applied to hindpaws ipsi- and contralateral to the recording probe (Fig. 2b). The graph illustrates two poststimulus time series for the whole region derived by averaging the time series of individual pixels in the image following equivalent noxious stimulation of the right and left hindpaws. Note a general darkening of the image when the right paw was pinched (see also Fig. 2a) compared with a general lightening when the left foot was pinched. Presumably, general systemic state changes induced by noxious stimulation should be largely independent of laterality.

(ii) Differential responses to auditory and visual stimuli were observed in data sequences simultaneously imaging the superior and inferior colliculus. These adjacent structures were chosen: (a) because of their differential sensory sensitivity—the superficial layers of the superior colliculus receive direct input from retinal ganglion cells (Fukuda and Iwama, 1978), while the inferior colliculus is the principal auditory structure in the midbrain (Coleman and Clerici, 1987)—and (b) because careful positioning of the optical probe permitted simultaneous recording of optical signals from both structures. Thus, with the blood vessel between the superior and inferior colliculus running approximately horizontally across the center of the image, the dorsal surface of the caudal superior colliculus was represented in the upper half of the image,

while the surface of the rostral inferior colliculus was in the lower half of the image (top left, Fig. 4a). Figure 4a shows, as expected, that the inferior colliculus was preferentially activated by auditory stimulation while the superior colliculus was more sensitive to visual stimuli (Fig. 4b). The image processing for these montages was identical to that described for the montage in Fig. 2a. The differential responses of the colliculi were particularly evident after the statistical procedures commonly applied to optical signals to reveal functional architecture in sensory systems (Blasdel and Salama, 1986; Bonhoeffer and Grinvald, 1993; Frostig *et al.*, 1990; Grinvald *et al.*, 1988, 1991) were applied to our images (Fig. 4c). Images from two trials were averaged for each condition. Each condition image was then normalized by dividing with a “cocktail image” formed from the sum of the condition images.

(iii) Direct electrical stimulation of collicular tissue imaged by the optical probe produced a modulation of the signal which was quantitatively related to stimulation intensity (Fig. 5). Figure 5a presents an averaged time series indicating the optical response to a 10-s train of cathodal 0.2-ms square wave pulses, 100 Hz, 200  $\mu$ A. It shows the low-frequency 0.1-Hz signal superimposed on the increase in intensity caused by direct electrical stimulation of the imaged tissue. The poststimulus increase in intensity can arise from at least two confounded sources: (a) hyperoxygenation due to increase inflow of arterial blood (LaManna *et al.*, 1987; Malonek and Grinvald, 1996) and (b) a change in image intensity produced by the oxidation of cytochrome aa3 (optical signals with similar time course were obtained by Jobsis *et al.*, 1977, recording at 590–605 nm following direct electrical stimulation of neural tissue). However, in rat brain at 620 nm there is an isobestic point for cytochrome oxidase absorption (Miyake *et al.*, 1991). Thus, at the longer wavelengths of illumination used in the present study ( $660 \pm 20$  nm) one would expect any image effects of cytochrome oxidation to be opposite to those produced by the inflow of oxygenated blood (i.e., reduce the image intensity). Figure 5b presents a graph showing that the change in temporal variance in the mean image following electrical stimulation was related to stimulation intensity in the range 50–400  $\mu$ A. Variance (amplitude squared) in the time series 25 s prior to the stimulation was subtracted from the 25-s poststimulation variance for each intensity. In a separate experiment, application of

**FIG. 2.** (a) Coherent spatiotemporal structure in a sequence of images recorded from left hindlimb motor cortex following noxious mechanical stimulation of the right hind paw of an anesthetized rat. (b) Control stimulation of the left (ipsilateral) hind paw yielded a consistently different response. (c) An averaged time series from the motor cortex of a second rat following similar noxious stimulation of the contralateral hind paw provided an example of a maintained step increase in gray level following stimulation.

**FIG. 3.** Optical responses of cat hippocampus during a transition from a period of slow wave (quiet) sleep to rapid eye movement (REM) sleep. (a) Mean gray level changes in the optical record occurring during the transition. (b) A montage of frames selected at 2-s intervals covering the transition between sleep states.

the local anesthetic, procaine, to the surface of the imaged structure significantly reduced the amplitude of the electrically induced optical response, but interestingly, some evidence of the low-frequency oscillation remained (Fig. 5c). In this preparation, we observed only the large increase in image intensity due to the hyperoxygenation of the tissue by the influx of fresh blood. Note that the time course of these responses can vary between experiments and is generally much slower (e.g., 20–30 s) than the rapid deoxygenation response reported in the functional mapping studies (<3 s) (Frostig *et al.*, 1990; Grinvald *et al.*, 1988, 1991). This overshoot in intensity is an order of magnitude greater than the reported deoxygenation responses which would be expected to decrease the intensity of the signal.

(iv) When the preparation was given a lethal overdose of barbiturate, both the response to electrical stimulation and the underlying 0.1-Hz signal decreased and vanished as the animal succumbed (data not shown).

In summary, the data show: (i) Reflectance signals from brain contain a large-amplitude 0.1-Hz oscillation which is present in both parenchyma and blood vessels; (ii) this signal may be modulated by local neural activity; however, in our data, it is superimposed on the image changes resulting from stimulus-induced neural activation; (iii) the low-frequency signal is neither spatially nor temporally homogeneous; (iv) the amplitude of this low-frequency “noise” is at least an order of magnitude greater than the differential mapping signals used to reveal functional architecture (Blasdel and Salama, 1986; Bonhoeffer and Grinvald, 1993; Frostig *et al.*, 1990; Grinvald *et al.*, 1988, 1991); and (v) the oscillation appears to be a general feature across species.

The important implication of these results for reflectance imaging (and other blood-related neuroimaging techniques, see below), is that a data capture methodology which uses repeating image acquisition intervals in the order of 10 s is potentially vulnerable to systematic sampling bias. Many optical imaging studies capture the first 3 s of poststimulus modulation, followed by a 7-s rest interval (Blasdel and Salama, 1986; Bonhoeffer and Grinvald, 1993; Frostig *et al.*, 1990; Grinvald *et al.*, 1988, 1991; Obermayer and Blasdel, 1993). Sampling at these rates could, in principle, induce aliasing artifacts which might be interpreted as stimulus-driven changes in the signal.

The strategy of collecting data immediately (<3 s) poststimulation certainly avoids problems arising from the low-resolution, large delayed increases in signal produced by hyperoxygenation or cytochrome oxidation. However, this strategy cannot avoid the interactions between stimulus-induced effects and the background 0.1-Hz modulation.

The strategy of subtracting data collected under

different stimulus conditions relies on the assumption that the effects of such noise or artifacts are evenly distributed between the different stimulus conditions and can therefore be cancelled from the data either by subtraction of one image from the other or by the alternative, but similar, strategy of dividing the mean image of one stimulus condition by the average of the images over all the stimulus conditions (Blasdel and Salama, 1986; Bonhoeffer and Grinvald, 1993). We have just completed an extensive simulation study which evaluated methods of analysis of optical signals (Mayhew and Zheng, manuscript in preparation). The results of this work show that the differencing strategy described above, though reasonably effective, is still vulnerable to spatial and temporal inhomogeneity in the low-frequency signal, in proportion to its amplitude. In our model, such inhomogeneities introduced distortion into the spatial structure of recovered functional maps even at relatively low amplitude. It is, therefore, necessary to characterise the 0.1-Hz oscillation and its relationship to neural activity, first to control for its impact on functional mapping investigations, but more importantly, to understand its role in the coupling of neural activity to regional blood flow.

The present results further demonstrate that the mechanisms underlying optical signals are complex. In particular, the manner in which the 0.1-Hz oscillation interacts with other components of the optical signals, including other hemodynamic components and conformational changes in the structure of neurones and glia (Cohen, 1973; Frostig *et al.*, 1990; Gozal *et al.*, 1993; Grinvald *et al.*, 1988, 1991; Poe *et al.*, 1994; Rector and Harper, 1991; Rector *et al.*, 1993; Tasaki and Byrne, 1994; Tasaki and Iwasa, 1982), clearly requires further research. For example, the mechanism of the peripheral 0.1-Hz signal measured in the capillary beds has been attributed to variation in hematocrit densities produced by modulated blood flow resulting from changes in arteriole diameter (Fagrell *et al.*, 1980). Morita *et al.* (1995) proposed a myogenic source for the oscillation; on the other hand, Golanov and colleagues (Golanov and Reis, 1995; Golanov *et al.*, 1994) present evidence for a neurogenic origin. Whatever the ultimate source of the 0.1-Hz signal, it remains to determine how it interacts with the other optical signal sources related to stimulation-induced neural activity. For example, the timing of stimulus presentation relative to the phase of the 0.1-Hz oscillation will interact critically with neurally induced hemodynamic response to stimulation. For the interpretation of image data sequences, it is important to develop a system model which can be used in the analysis to decouple the baseline neuro-hemodynamics from the experimental signal data stream.

These results have significant implications for functional magnetic resonance imaging (fMRI) and positron

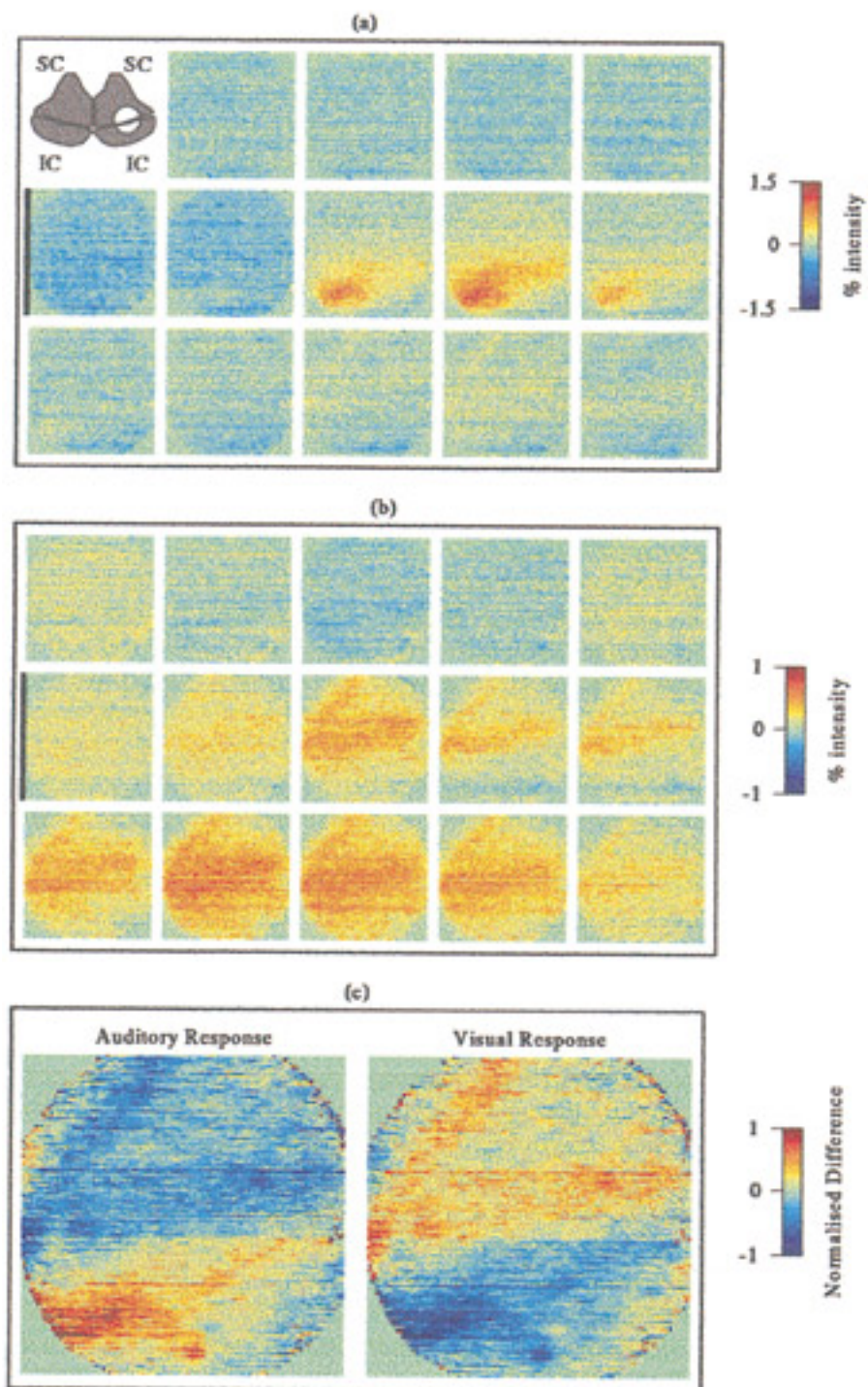


**FIG. 4.** Further examples of optical responses induced by sensory stimulation and physiological state changes. (a) A peristimulus montage showing reflectance changes of the rat superior and inferior colliculus to auditory stimulation. The sensory stimuli were administered at the beginning of the second row of images signified by black bar. Note a differential response to the auditory stimulus from the inferior colliculus. (b) An identical montage showing the response of the superior and inferior colliculus to a visual stimulus. Note a differential response to the visual stimulus from the superior colliculus. (c) Single-condition maps created using an analysis procedure used widely in the optical imaging literature (see text).

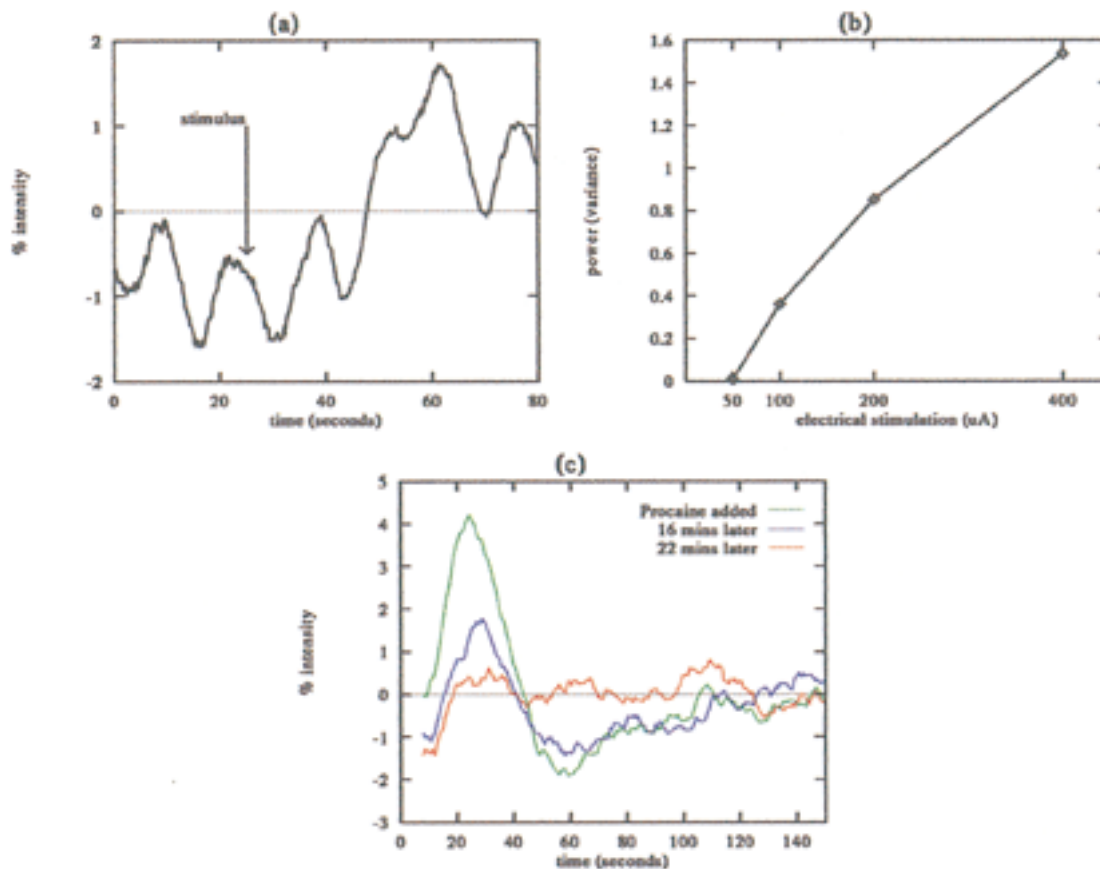


**FIG. 5.** Electrical stimulation of rat colliculus produced a modulation of the 0.1-Hz signal which was related to stimulation intensity. Subsequent application of local anesthetic suppressed the response to electrical stimulation. (a) An averaged time series indicating the optical response to a 10-s train of electrical stimulation applied to the imaged tissue. (b) The change in temporal variance (amplitude of oscillation squared) in the mean image following electrical stimulation was related to stimulation intensity. (c) Successive time series illustrating the response to electrical stimulation (5-s train of 0.5-ms cathodal square wave pulses; 800 mA; 100 Hz) following the direct application of the local anesthetic, procaine, to the surface of the superior colliculus.

emission tomography (PET). The presence of 0.1-Hz vasomotion-like oscillation in the brain may induce various forms of aliasing in fMRI and PET images which are typically acquired at low sample rates. The sampling rates of even the new generation of fast echo-planar fMRI devices are below, or dangerously close to, the aliasing (Nyquist) frequency of the vasomotion signal (Fox *et al.*, 1988; Friston *et al.*, 1994; Kwong *et al.*, 1992; Le Bihan and Karni, 1995; Sereno *et al.*, 1995). The 0.1-Hz oscillations may be involved in the well-known low spatial frequency “banding” artifacts that can occur in fMRI difference images which Cohen *et al.* (1993) suggest may result from changes in regional blood flow occurring during capture. Indeed, the presence of a low-frequency signal in a 1024 sample fMRI data sequence has been reported (Weisskoff *et al.*, 1993). It seems likely that this signal was the same as the 0.1-Hz source recently identified in an fMRI data stream by P. Mitra (personal communication). Friston *et al.* (1994) exploit an explicit model of the neurohemodynamic temporal response in their proposed

statistical analysis of fMRI data. Whether the use of their generalized linear model approach will be effective in separating the effects of such 0.1-Hz signals from the analysis (e.g., by including it as a confound in the design matrix) awaits further evaluation.

The spatial and temporal resolution afforded by optical imaging is a significant advance for monitoring the modulation of cerebral microcirculation. Controversy still exists on the source of the oscillatory component of the signal measured by LDF meters. For example, it has been reported that “pronounced vasodilation leads to a total abolition of vasomotion” (Morita *et al.*, 1995). One implication is that the modulation of flow is a side effect of the vasodilatory activity of the larger vessels in the microvasculature and that when these vessels are fully dilated, there is no modulation in the capillary beds. On the other hand, Golanov *et al.* (1994) proposed a neurogenic origin for at least one class of low-frequency oscillations in cortex. The present optical imaging technique may assist in the resolution of this issue since it enables fine spatial resolution

measurements of all aspects of the microcirculation simultaneously.

Finally, future applications could quantitatively assess spatiotemporal dynamics of interaction between the brain and its blood supply and address the issue of whether the structure of underlying capillary beds reflects the functional architecture of the neuropil they service, as suggested by Cox *et al.* (1993). The temporal and spatial dynamics of neurochemical systems, e.g., the role of nitric oxide in regional cerebral blood flow, are likely to be at the forefront of these investigations (Dirnagl *et al.*, 1993; Garthwaite and Boulton, 1995). The resulting information promises to assist interpretation of data from other imaging techniques which exploit local changes in metabolic activity and control of regional blood flow.

### ACKNOWLEDGMENTS

Supported by Wellcome Trust Grant 038011/Z/93 to P.R., HL-22418 to R.M.H., and MRC Grant G9408599N to G.W.M.W. Sincere thanks to Philip Bashum of Perimed International for the loan of the Laser Doppler Flow meter (Model 4001) and his technical support and to Marion Simkins for proofreading the manuscript.

### REFERENCES

- Blasdel, G. G., and Salama, G. 1986. Voltage-sensitive dyes reveal a modular organization in monkey striate cortex. *Nature* **321**:579–585.
- Bonhoeffer, T., and Grinvald, A. 1993. The layout of iso-orientation domains in area 18 of cat visual cortex: Optical imaging reveals a pinwheel-like organization. *J. Neurosci.* **13**:4157–4180.
- Carmona, R. A., Hwang, W. L., and Frostig, R. D. 1995. Wavelet analysis for brain-function imaging. *IEEE Trans. Med. Imaging* **14**:556–564.
- Cohen, J. D., Noll, D. C., and Schneider, W. 1993. Functional magnetic resonance imaging: Overview and methods for psychological research. *Behav. Res. Methods Instrum. Comput.* **25**:101–113.
- Cohen, L. B. 1973. Changes in neuron structure during action potential propagation and synaptic transmission. *Physiol. Rev.* **53**:373–418.
- Colantuoni, A., Bertuglia, S., and Intaglietta, M. 1994. Microvascular vasomotion: Origin of laser doppler flux motion. *Int. J. Microcirc.* **14**:151–158.
- Coleman, J. R., and Clerici, W. J. 1987. Sources of projections to subdivisions of the inferior colliculus in the rat. *J. Comp. Neurol.* **262**:215–226.
- Cox, S. B., Woolsey, T. A., and Rovainen, C. M. 1993. Localized dynamic changes in cortical blood flow with whisker stimulation corresponds to matched vascular and neuronal architecture of rat barrels. *J. Cereb. Blood Flow Metab.* **13**:899–913.
- Dean, P., Redgrave, P., and Lewis, G. 1982. Locomotor activity of rats in open field after microinjections of procaine into superior colliculus or underlying reticular formation. *Behav. Brain Res.* **5**:175–187.
- Dirnagl, U., Kaplan, B., Jacewicz, M., and Pulsinelli, W. 1989. Continuous measurement of cerebral cortical blood flow by laser-Doppler flowmetry in a rat stroke model. *J. Cereb. Blood Flow Metab.* **9**:589–596.
- Dirnagl, G., Lindauer, U., and Villringer, A. 1993. Role of nitric oxide in the coupling of cerebral blood flow to neuronal activation in rats. *Neurosci. Lett.* **149**:43–46.
- Fagrell, B., Intaglietta, M., and Ostergren, J. 1980. Relative hematocrit in human skin capillaries and its relation to capillary blood flow velocity. *Microvasc. Res.* **20**:327–335.
- Fox, P. T., Raichle, M. E., Minton, M. A., and Dence, C. 1988. Non-oxidative glucose consumption during focal neurophysiologic activity. *Science* **241**:462–464.
- Friston, K. J., Jezzard, P., and Turner, R. 1994. Analysis of functional MRI time-series. *Hum. Brain Mapping* **1**:153–171.
- Frostig, R. D., Lieke, E. E., Ts'o, D., and Grinvald, A. 1990. Cortical functional architecture and local coupling between neuronal activity and the microcirculation revealed by in vivo high-resolution optical imaging of intrinsic signals. *Proc. Natl. Acad. Sci. USA* **87**:6082–6086.
- Fukuda, Y., and Iwama, K. 1978. Visual receptive-field properties of single cells in the rat superior colliculus. *Jpn. J. Physiol.* **28**:385–400.
- Garthwaite, J., and Boulton, C. L. 1995. Nitric oxide signalling in the central nervous system. *Annu. Rev. Physiol.* **57**:683–706.
- Golanov, E. V., and Reis, D. J. 1995. Vasodilation evoked from medulla and cerebellum is coupled to bursts of cortical EEG activity in rats. *Am. J. Physiol.* **268**:R454–R467.
- Golanov, E. V., Yamamoto, S., and Reis, D. J. 1994. Spontaneous waves of cerebral blood flow associated with a pattern of electrocortical activity. *Am. J. Physiol.* **266**:R204–214.
- Gozal, D., Dong, X.-W., Rector, D. M., and Harper, R. M. 1993. Optical imaging of the ventral medullary surface of cats: Hypoxia-induced differences in neural activation. *J. Appl. Physiol.* **74**:1658–1665.
- Grinvald, A., Frostig, R. D., Lieke, E., and Hildesheim, R. 1988. Optical imaging of neuronal activity. *Physiol. Rev.* **68**:1285–1365.
- Grinvald, A., Frostig, R. D., Siegel, R. M., and Bartfeld, E. 1991. High-resolution optical imaging of functional brain architecture in the awake monkey. *Proc. Natl. Acad. Sci. USA* **88**:11559–11563.
- Hill, D. K., and Keynes, R. D. 1949. Opacity changes in the stimulated nerve. *J. Physiol.* **108**:278–281.
- Jobsis, F. F., Keizer, J. H., LaManna, J. C., and Rosenthal, M. 1977. Reflectance spectrophotometry of cytochrome aa3 in vivo. *J. Appl. Physiol.: Respir., Environ. Exercise Physiol.* **43**:858–872.
- Kwong, K. K., Belliveau, J. W., Chesler, D. A., Goldberg, I. E., Weisskoff, R. M., Poncelet, B. P., Kennedy, D. N., Hoppel, B. E., Cohen, M. S., Turner, R., Cheng, H.-M., Brady, T. J., and Rosen, B. R. 1992. Dynamic magnetic resonance imaging of human brain activity during primary sensory stimulation. *Proc. Natl. Acad. Sci. USA* **89**:5675–5679.
- LaManna, J. C., Sick, T. J., Pikarsky, S. M., and Rosenthal, M. 1987. Detection of an oxidizable fraction of cytochrome oxidase in intact rat brain. *Am. J. Physiol.* **253**:C477–C483.
- Le Bihan, D., and Karni, A. 1995. Applications of magnetic resonance imaging to the study of human brain function. *Curr. Opin. Neurobiol.* **5**:231–237.
- Lipton, P. 1973. Effects of membrane depolarization on light scattering by cerebral cortical slices. *J. Physiol.* **231**:365–383.
- MacVicar, B. A., and Hochman, D. 1991. Imaging of synaptically evoked intrinsic signals in hippocampal slices. *J. Neurosci.* **11**:1458–1469.
- Malonek, D., and Grinvald, A. 1996. Interactions between electrical activity and cortical microcirculation revealed by imaging spectroscopy: implications for functional brain mapping. *Science* **272**:551–554.
- Morita, Y., Hardebo, J. E., and Bouskela, E. 1995. Influence of cerebrovascular sympathetic, parasympathetic, and sensory nerves

- on autoregulation and spontaneous vasomotion. *Acta Physiol. Scand.* **154**:121–130.
- Neafsey, E. J., Bold, E. L., Haas, G., Hurley-Gius, K. M., Quirk, G., Sievert, C. F., and Terreberry, R. R. 1986. The organization of the rat motor cortex; a microstimulation mapping study. *Brain Res. Rev.* **11**:77–96.
- Obermayer, K., and Blasdel, G. G. 1993. Geometry of orientation and ocular dominance columns in monkey striate cortex. *J. Neurosci.* **13**:4114–4129.
- Poe, G. R., Rector, D. M., and Harper, R. M. 1994. Hippocampal reflected optical patterns during sleep and waking states in the freely behaving cat. *J. Neurosci.* **14**:2933–2942.
- Ratzlaff, E. H., and Grinvald, A. 1991. A tandem-lens epifluorescence macroscope: Hundred-fold brightness advantage for wide-field imaging. *J. Neurosci. Methods* **36**:127–137.
- Rector, D., and Harper, R. M. 1991. Imaging of hippocampal neural activity in freely behaving animals. *Behav. Brain Res.* **42**:143–149.
- Rector, D. M., Poe, G. R., and Harper, R. M. 1993. Fibre optic imaging of subcortical neural tissue in freely behaving animals. *Adv. Exp. Med. Biol.* **333**:81–86.
- Sereno, M. I., Dale, A. M., Reppas, J. B., Kwong, K. K., Belliveau, J. W., Brady, T. J., Rosen, B. R., and Tootell, R. B. H. 1995. Borders of multiple visual areas in humans revealed by functional magnetic resonance imaging. *Science* **268**:889–893.
- Sundberg, S. 1984. Acute effects and long-term variations in skin blood flow measured with Laser Doppler flowmetry. *Scand. J. Clin. Lab. Invest.* **44**:341–345.
- Tasaki, I., and Byrne, P. M. 1994. Optical changes during nerve excitation—interpretation on the basis of rapid structural changes in the superficial gel layer of nerve fibers. *Physiol. Chem. Phys. Med. NMR.* **26**:101–110.
- Tasaki, I., and Iwasa, K. 1982. Further studies of rapid mechanical changes in squid giant axon associated with action potential production. *Jpn. J. Physiol.* **32**:505–518.
- Ts'o, D. Y., Frostig, R. D., Lieke, E. E., and Grinvald, A. 1990. Functional organization of primate visual cortex revealed by high resolution optical imaging. *Science* **249**:417–420.
- Weisskoff, R. M., Baker, J., Belliveau, J., Davis, T. L., Kwong, K. K., Cohen, M. S., and Rosen, B. R. 1993. Power spectrum analysis of functionally-weighted MR-data: What's in the noise. *Soc. Magn. Reson. Med.* **XII**:7.
- Zilles, K. and Wree, A. 1985. Cortex: Areal and laminar structure. In *The Rat Nervous System: Vol 1. Forebrain and Midbrain*. G. Paxinos, Ed., pp. 375–415. Academic Press, Sydney.